Integrated Aerodynamic/Structural Design of a Sailplane Wing

B. Grossman,* Z. Gurdal,† G. J. Strauch,‡ W. M. Eppard,‡ and R. T. Haftka*
Virginia Polytechnic Institute and State University, Blacksburg, Virginia

The objective of this research is an investigation of the techniques and payoffs of integrated aircraft design. In particular, we studied the interaction of aerodynamic and structural design for a simple aircraft configuration—a sailplane wing. Utilizing elementary analysis tools, lifting-line theory, beam analysis, the geometry (planform, twist), along with the composite-material structural sizes (skin thickness, spar cap, and web thicknesses), comprising 25–35 variables, were designed subject to aeroelastic, structural, and aerodynamic constraints. We investigated two design procedures. One is the Sequential Design, where the aerodynamic geometry is designed to maximize the performance (defined as the average cross-country speed), followed by a structural/aeroelastic design to minimize the weight. The weight is input to the aerodynamic analysis, and the process continues iteratively. The second procedure is the Integrated Design. Here we simultaneously design the aerodynamics and the structure. All design quantities are determined simultaneously in a single optimization to maximize performance or minimize weight. In all cases, the integrated design was superior in terms of performance or weight to the sequential design. The integrated designs were characterized by less rigid, higher-aspect ratio wings that utilized favorable aerodynamic/structural interactions.

I. Introduction

AIRCRAFT design requires the integration of several disciplines, such as aerodynamics, structures, controls, and propulsion. In the traditional design process, these disciplines are integrated only during the preliminary design phase, where simple analytical tools are used to make decisions concerning overall shape and size parameters. After this phase, the complexity of the analysis required for individual discipline design decisions typically discourages design integration except in crisis situations. For example, if the wing structural design results in excessive weight, the aerodynamic design may need to be altered to provide load relief.

The introduction of composite materials into aircraft structures provides an incentive to increase the integration of the aerodynamic design and structural design of aircraft wings. This is due to the potential for controlling the structural deformations of the wings by tailoring the orientation of the composite fibers. This so-called aeroelastic tailoring can be used to improve aerodynamic performance (e.g., Refs. 1 and 2) for controlling load distribution or for preventing aeroelastic instabilities (see Refs. 3 and 4 for additional references).

Together with increased interest in tailoring the structure to control aerodynamic loads, there is a continued interest in modifying the aerodynamic load distribution on a wing to alleviate stresses (see Ref. 5 for additional references). The basic approach is to shift the loads inboard compared to the optimal aerodynamic distribution in order to allow a larger span for a given structural weight, which in turn improves the aerodynamic performance. McGeer's work[5] improved on the realism of the wing model, including compressibility and sweep effects, considering simultaneously both cruise and maneuver conditions and including load inertia relief due to the wing weight.

The purpose of the present work is to perform a pilot study of the integration of aerodynamic and structural wing design that accounts for both interactions. The emphasis in the present study is on the techniques required for design integration and the assessment of the payoffs in terms of improved performance. This is done by comparing an integrated design technique to a more traditional iterative technique for a simple wing.

For the sake of simplicity, a sailplane wing was selected for the study. A sailplane travels at low speeds; it has no thrust, engines, or fuel to account for, and it has a simple mission. The mission studied here involves climbing in a thermal and then cruising to the next thermal while losing the altitude previously gained. The performance index in the mission was the average cross-country speed.

An existing sailplane with readily available detailed design information was sought for verification of the design procedures. A 13.5-m sailplane called RP-2, designed and built at Rensselaer Polytechnic Institute, was chosen to meet these requirements. The required design information was acquired from Refs. 6–8, and some characteristic data is given in Table 1.

II. Modeling of the Sailplane

Performance

The mission chosen is for the glider to climb to a height H in a prescribed thermal, then to cruise a distance D while losing altitude H, as depicted in Fig. 1. The performance index to be maximized for this mission is the average cross-country speed derived later. Carmichael and Horstmann thermal profiles of various strengths such as those used by Helwig[9] were considered.

The net rate of climb of the sailplane in the thermal is given by

$$V_c(R) = V_{\text{thermal}}(R) - V_{sc} \tag{1}$$

where V_{thermal} is the upward velocity of the air at a distance R from the center of the thermal and V_c is the rate of climb in the thermal. The sink speed in the thermal V_{sc}, can be obtained in terms of lift and drag coefficients during the climb C_{L_c} and C_{D_c}, the wing area S, and the total weight W by assuming a small downward flight-path angle as

$$V_{sc} = \frac{C_{D_c}}{C_{L_c}^{1.5}}\left[1 - \left(\frac{2W}{\rho S C_{L_c} g R}\right)^2\right]^{-0.75}\left(\frac{2W}{\rho S}\right)^{0.5} \tag{2}$$

where ρ is the air mass density and g the gravitational acceleration.

The cruise speed is given in terms of the cruise lift coefficient C_L as

$$V = (2W/\rho S C_L)^{0.5} \tag{3}$$

Presented as Paper 86-2623 at the AIAA Aircraft Systems, Design and Technology Meeting, Dayton, OH, Oct. 20–22, 1986; received June 6, 1987; revision received Dec. 12, 1987.

*Professor of Aerospace and Ocean Engineering. Member AIAA.
†Assistant Professor of Engineering Science and Mechanics. Member AIAA.
‡Graduate Student.

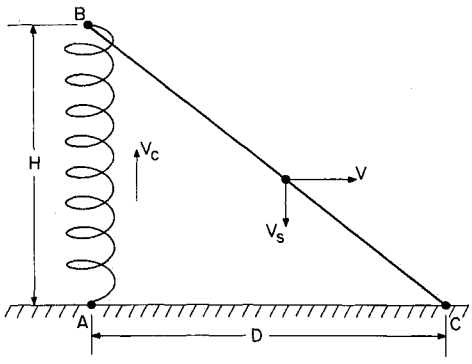

Fig. 1 Sailplane mission profile.

Table 1 Characteristic data for RP-2 glider

Overall:	
Span	13.5 m
Length	6.6 m
Height	1.25 m
Wing:	
Area	11.1 sq. m
Aspect Ratio	16.4
Section	BOAF-163
Vertical stabilizer:	
Span	1.25 m
Area	0.5 sq. m
Section profile	FX-L-111-142
Horizontal stabilizer:	
Span	2.5 m
Area	1.0 sq. m
Section profile	FX-L-111-142
Performance at gross weight of 160 kg (353 lbs):	
Stall speed w/o flaps	47 km/h
Min. sink rate	0.53 m/s
Max. glide ratio	28 at 61 km/h
Empty weight (estimated):	78 kg

and the sink speed during cruise V_s, can be obtained in terms of the cruise lift and drag coefficients C_L, C_D by assuming a small downward flight-path angle as

$$V_s = \frac{C_D}{C_L^{1.5}}(2W/\rho S)^{0.5} \tag{4}$$

The cross-country speed is determined from the mission profile as depicted in Fig. 1. We define this speed as

$$V_R = D/t \tag{5}$$

where t is the total time of travel between points A and C and D is the horizontal distance from A to C. Equating the height gained in the climb portion to that lost in the cruise portion, we obtain

$$V_R = \frac{VV_c}{V_c + V_s} \tag{6}$$

This average cross-country speed V_R serves as the mission performance index for the design study.

Aerodynamic Analysis

The aerodynamic loads were found using lifting-line techniques. The lifting forces and the induced drag were found using the monoplane equation, e.g., Bertin and Smith.[10]

The sailplane wing semispan was divided into eight sections, and stations were defined at the midpoint of each section.

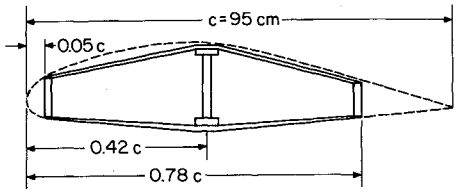

Fig. 2 Typical cross-section of wing element.

From the geometry of the wing and the angles of attack at each station, a system of eight equations in eight unknowns, denoted A_1–A_8, was generated by applying the monoplane equation at each station. Once the constant A_n were calculated, the total lift coefficient, the local lift coefficients, and the induced drag coefficient could be calculated.

The profile drag coefficients at each station were found using the local lift coefficients and the C_ℓ–C_d curve for the given airfoil section. The section used was the Boeing BoAR-80-RPVT-16B. The profile drag coefficients were assumed to be constant over each section of the wing. The total drag coefficient was found by summing each local profile drag coefficient mutiplied by the respective area of that section and then dividing by the total wing area.

The parasite drag coefficient of the fuselage and tails was treated as a function of the wing area as in Helwig:[9]

$$C_{D_O} = \frac{\text{const}}{S} \tag{7}$$

where the constant (sometimes referred to as an equivalent flat-plate area) depends on the type of aircraft. For our sailplane analysis, a value of 0.08 m^2 was used in the preceding parasite drag equation.

Structural Analysis

The structural analysis was based on a beam model. The wing was divided into eight constant cross-section elements along the span. Each element was an untapered two-cell box beam that conformed with the shape of the airfoil at the spanwise center of the section (see Fig. 2). The main spar between the two cells was an I beam with spar caps built of unidirectional graphite fibers oriented spanwise. The spar web and the skin were a sandwich construction of Kevlar face sheets with a foam core, with the Kevlar fibers oriented at ± 45 deg with respect to the spanwise direction. Because the wing had a symmetric skin layup, there was no bending-torsion coupling. All the bending loads were carried by the main spar and by assumed spanwise stringers obtained by lumping the axial stiffness of the total skin at five selected locations on each face of the wing. The shear flow distribution in the skin was, therefore, assumed to be constant between the stringers.

The parameters that described the global structural behavior were the modulus-weighted bending rigidity EI and torsional rigidity GJ of each element of the wing. The torsional rigidities of each element as well as the location of the shear center of each element were obtained by carrying a shear flow analysis under the bending, twisting, and shearing loads. Once the modulus-weighted section properties (EI and GJ) were calculated, the structural displacements were computed by numerical integration using weighting matrices and structural influence coefficients. The divergence speed was calculated using the homogeneous form of the matrix equations. Finally, the total weight of the plane was also calculated, with the fuselage and tail section weight assumed to be a constant 130 kg. This was the weight of the RP-2 with a pilot minus the weight of the wings.

Aeroelastic Analysis

The aeroelastic analysis is based on the equation of static torsional equilibrium of a straight wing about its elastic axis considering only the effects of torsional deformations on the lift distribution. The equation is written in the classical

Table 2 Design variables

3 performance design variables	1. Angle of attack at the root during the turn
	2. Angle of attack at the root during cruise
	3. Raduis of the turn
6 geometric design variables	4. Angle of twist at the break relative to the root
	5. Angle of twist at the tip relative to the root
	6. Chord length at the root
	7. Chord length at the break
	8. Chord length at the tip
	9. Distance to the break
24 structural design variables	10–17. Spar cap thickness for each wing section
	18–25. Spar web thickness for each wing section
	26–33. Skin thickness for each wing section

Semispan was also used as a design variable for one design.

Table 3 Design constraints

3 stall constraints during turning maneuver	1. No stall at the root
	2. No stall at the break
	3. No stall at the tip
3 performance constraints	4. Bank angle less than 50 deg
	5. Climb speed greater than zero
	6. Minimum divergence speed
24 structural constraints (at 43 m/s, 5.9 g)	7–14. Maximum spar cap strain for each wing section, 0.3%
	15–22. Maximum shear stress for each wing section, web shear <600 N/mm^2
	23–30. Wing skin must satisfy Tsai-Hill strength constraint for each wing section

Minimum average cross-country speed was also used as a constraint for weight minimized designs.

Bisplinghoff[11] notation expressing the elastic change in local angle of attack α^e as the sum of three terms,

$$\{\alpha^e\} = q[E][c]\{C_L^e\} + \{f\} + \alpha^e(0)\{1\} \tag{8}$$

where curly brackets are used to denote vectors of a quantity at spanwise wing stations and straight brackets are used for matrices. The first term on the right-hand side of Eq. (8) represents the elastic angle of attack due to the additional lift generated by α^e, where q is the dynamic pressure, E is a flexibility matrix such that its element E_{ij} represents the twist angle in station i due to a unit lift at station j, $[c]$ is a diagonal matrix of chord lengths, and C_L^e is the lift coefficient due to α^e. The second term, $\{f\}$, represents the contribution to α^e due to the lift and aerodynamic moment acting on a rigid wing and to the inertia forces. The third term represents pilot correction of the root angle of attack $\alpha^e(0)$ to maintain constant total lift, and $\{1\}$ denotes a vector of ones. This condition of constant total lift is expressed as

$$\{1\}^T[W][c]\{C_L^e\} = 0 \tag{9}$$

where $[W]$ is a diagonal matrix of weighting values related to the length of the spanwise section associated with each station.

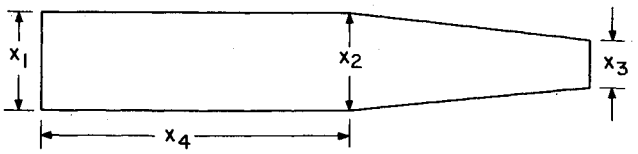

Fig. 3 Planform geometry variables.

The elastic lift increment C_L^e is given as

$$\{C_L^e\} = [A]\{\alpha^e\} \tag{10}$$

where the element A_{ij} of the matrix A represents the change in lift coefficient in section i due to a unit twist angle at station j.

Equations (8–10) are solved together for α^e and C_L^e. Also, by setting $\{f\} = 0$ and $\alpha^e(0) = 0$, Eq. (8) becomes an eigenvalue problem, with the dynamic pressure q being the eigenvalue. The lowest eigenvalue represents the aeroelastic divergence speed.

III. Design of the Wing

Variables and Constraints

The sailplane wing design involved 33 or 34 design variables (see Table 2) and 30 or 31 constraints (see Table 3) depending on the objective function used. The wing planform was defined by chord lengths at the root tip and at a point in between denoted the break, and the spanwise coordinate of the break. The chord lengths varied linearly from root to break and from break to tip, as depicted in Fig. 3. The built-in twist was defined by its values at the break and the tip, with the twist varying linearly from root to break and from break to tip. The angles of attack at the root during the turning maneuver and during the cruise portion of the flight, along with the radius of the turn, are included as performance design variables. The spar cap thicknesses, spar web thicknesses, and the skin thicknesses at each of eight spanwise sections were the structural design variables.

The aerodynamic constraints consisted of a maximum bank angle, a minimum climb speed, no stalling of the wing at any section, and, for some cases, a performance constraint. The stall condition was enforced by requiring local section lift coefficients to be below the two-dimensional section stall value of 1.4. The structural constraints were imposed at a high-speed pullup maneuver, 5.3 g at 43 m/s. Limits were imposed on stresses in the spar webs and the skin, strains in the spar caps, and static divergence speed. (A flutter constraint was not considered.)

Design Procedures

Two design procedures were compared: a sequential, iterative procedure where the structural and aerodynamic optimizations were performed separately, and an integrated procedure where the entire design was obtained in one optimization. In the iterative, sequential procedure, the wing shape was first optimized for maximum cross-country speed using the planform and performance variables. This optimization was performed for a rigid wing with a given weight and was subject to the aerodynamic constraints described earlier. The optimized wing shape was then used for a structural optimization that minimized the weight of the wing by varying the structural variables while satisfying the structural constraints. The process was restarted by performing the aerodynamic optimization with the new weight. The iterative process continued until the difference between the weight used for the aerodynamic optimization and the optimized weight obtained by the structural optimization dropped below 0.2%. To correct for aeroelastic effects, this solution was used in another program that optimized the cross-country speed by varying only the performance variables while taking the effects of wing deformations on the performance into account. A schematic of the sequential, iterative procedure is shown in Fig. 4.

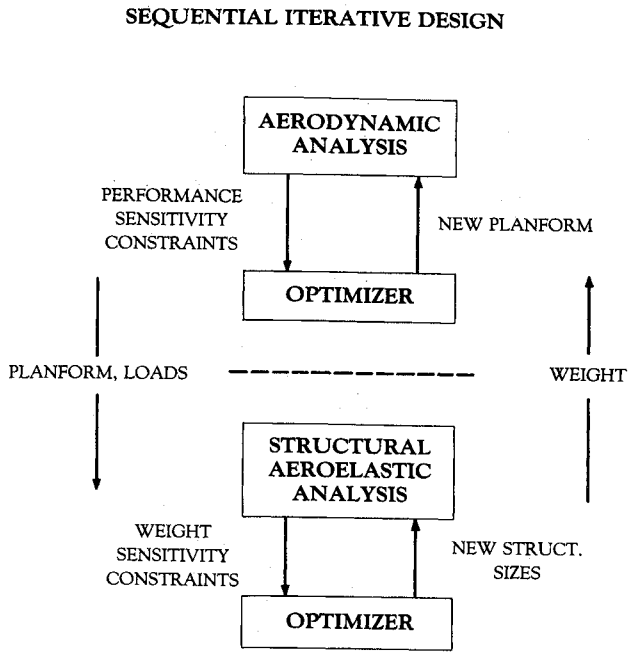

Fig. 4 Schematic of iterative, sequential design procedure.

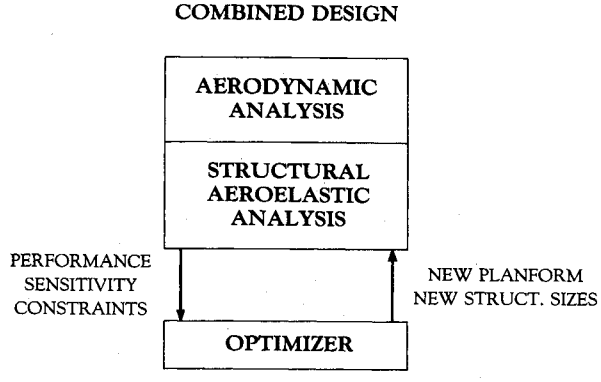

Fig. 5 Schematic of the integrated design procedure.

The integrated design procedure combined forms of all the above programs into one. The schematic of the process is shown in Fig. 5. The cross-country speed was maximized by varying all the performance, aerodynamic, and structural design variables at the same time. This allowed changes in the weight and the effects of wing deformations on the performance to be accounted for at all times during the optimization process. A second integrated design procedure was introduced where the weight was minimized with the additional constraint of a minimum cross-country speed requirement.

Optimization Technique

The program used for the optimization process was NEWSUMT-A.[12,13] The basic algorithm is the sequence of unconstrained minimization technique using penalty functions to account for constraints and Newton's method with approximate derivatives for unconstrained function minimizations.

Problems are formulated in terms of design variables x_j, $j = 1,...n_v$, as

Minimize

$$f(x_1,x_2,...,x_{n_v})$$

Subject to

$$g_q(x_1,x_2,...,x_{n_v}) \geq 0 \quad q = 1,2,...,n_{\text{ineq}}$$
$$h_q(x_1,x_2,...,x_{n_v}) = 0 \quad q = 1,2,...,n_{\text{eq}}$$

Table 4 Design results

	Iterated sequential	Integrated design	Weight minimization	RP-2 baseline
Cross-country speed (m/s)	3.44	3.48	3.44	3.35
Mass of one wing (kg)	13.0	12.5	11.6	14.2
Chord length				
root	100	105	105	95
break (cm)	100	98	98	95
tip	41	38	36	50
Distance to break (cm)	315	249	245	300
Twist (deg)				
break	0.23	0.16	0.15	0.0
tip	−0.22	−0.32	−0.01	−1.5
Aspect ratio	15.9	15.5	16.8	16.2
Wing area (m^2)	11.5	11.1	11.0	11.2

Thermal strength 0.9 m/s, span 13.5 m.

and the side bound on the design variables

$$x_j^{(\ell)} \leq x_j \leq x_j^{(u)} \qquad j = 1,2,...,n_v$$

where the objective functions $f(x)$, equality constraints $h_q(x)$, and inequality constraints $g_q(x)$ are continuous and differentiable real functions.

NEWSUMT-A systematically modifies an initial design vector while generating a sequence of vectors x^i so that $f(x)$ decreases or the degree of constraint satisfaction is improved. This sequence of vectors x converges to a solution x^* where the constraint violation is very small and $f(x^*)$ is at least a local minimum.

IV. Results and Discussion

We performed a series of design studies for sailplane wings in order to evaluate differences in the two design processes. The strength of the thermal was an input parameter, and the results were found to be highly sensitive to this strength. Because sailplanes depend on their weight for speed during cruise, they often carry ballast to increase their cross-country speed. This is done when the thermal used to climb to altitude is strong enough to offset the loss in climb speed due to the extra weight by the gain in cruise speed. However, in normal airplanes, minimum weight is usually desirable for maximum performance. Therefore, the thermal profile was initially chosen to be weak enough so that the sailplane weight was more critical during the climbing portion of the mission than during the cruising portion. An extremely weak Horstmann thermal profile was chosen whose strength varied outwards linearly from 0.9 m/s at its center.

In the first series of designs, the wing span was set at 13.5 m, as in the RP-2 design. Three designs were generated. A sequential, iterative design, an integrated design maximizing cross-country speed, and an integrated design minimizing weight subject to a minimum cross-country speed requirement equal to that obtained by the iterative design. The results and the corresponding values for the RP-2 are shown in Table 4. All these designs had better performance and lower weight than the RP-2 design. However, the RP-2 was not a fully optimized sailplane, and its design was not based on the same very weak thermal profile. The increase in performance of the integrated as compared to the iterative design was only 1%, with a 4% reduction in weight. The integrated minimum-weight design had a weight 11% lower than that of the iterative design with the same cross-country speed.

Table 5 Span design trends

	Span (m)	Cross-country speed (m/s)	Mass of one wing (kg)	Aspect ratio	Wing area (sq. m)
Sequential	13.5	5.15	12.6	16.2	11.2
Integrated	13.5	5.20	12.5	16.5	11.1
Sequential	20.0	8.21	25.7	26.3	15.2
Integrated	20.0	8.47	27.5	26.6	15.1
Sequential	25.0	6.23	41.7	44.3	20.3
Integrated	25.0	9.43	72.4	35.8	25.1
Span free design	27.75	9.95	76.0	38.1	20.2

Thermal strength 1.0 m/s

Table 6 Thermal strength effects

	Thermal strength (m/s)	Cross-country speed (m/s)	Mass of one wing (kg)	Aspect ratio	Wing area (sq. m)
Sequential	0.90	3.44	13.0	15.9	11.5
Integrated	0.90	3.48	12.5	16.5	11.1
Sequential	1.00	5.15	12.6	16.2	11.1
Integrated	1.00	5.20	12.5	16.5	11.0
Sequential	1.22	7.85	12.1	16.9	10.8
Integrated	1.22	7.88	12.2	17.4	10.5
Sequential	2.0	12.21	38.3	17.0	10.8
Integrated	2.0	13.46	46.9	18.2	10.1

The large effect on weight of the integrated design as compared to the small effect on performance is due to an imbalance between the two interactions in the structural and aerodynamic design. The first interaction allows changing aerodynamic load distributions to reduce stresses. The design variables employed in the present study allow substantial freedom to benefit from this interaction to reduce structural weight. The second interaction is taking advantage of structural deformations to improve performance. This effect is very weak in the present problem because of the relatively low g at the climb phase and because the composite skins were not utilized to obtain strong bending-torsion coupling.

The results in Table 4 also indicate a trend where a larger portion of the lift is moved inboard as the weight becomes lower by introducing more downwash and reducing the chord at the tip, as well as reducing the distance to the break. In addition, as the weight decreases, the wing also becomes more flexible.

The next series of designs was made for varying wing spans with a 1 m/s Horstmann thermal profile. Iterated and integrated maximized cross-country speed designs obtained for spans of 13.5, 20, and 25 m and an integrated design with the span as an additional design variable are shown in Table 5. The difference between the iterative and integrated designs became more apparent as the span became greater. The integrated designs had higher weights because as the span increased, the wing area increased, and the thermal, which was weak for the original designs, was now strong enough for these larger-area designs, so that the weight was no longer critical in the climb. Minimum weight no longer meant higher cross-country speed. This trend was found by the integrated design, but the iterative design still automatically assumed that minimum weight was always the best direction to take. To make the iterative designs more comparable to the integrated designs for strong thermals, nonstructural weight (ballast) could be added as an additional design variable.

One integrated design was obtained with the span as a design variable. This resulted in an optimal wing span of 27.75 m, with an aspect ratio of 38.1 and a mass for one wing of 76.0 k. These parameters combined to yield a high cross-country speed of 9.95 m/s. A wing with this large a span and such a high aspect ratio may not be a practical design for a marketable sailplane, but it does present a finite limit to the benefits gained from the favorable trends found with the integrated procedure. In addition, we have not accounted for the change in some aircraft parameters, such as the tail area, with changes in the wing span. This omission should not significantly affect the design trends we have observed.

Another design study was performed to assess how sensitive the results were to the thermal strength. An iterated, sequential design and an integrated design for a span of 13.5 m was made for thermal strengths of 0.9, 1.0, 1.22, and 2.0 m/s at the center. These results are shown in Table 6. The thermals with 1.22- and 2.0-m/s airspeed at its center were considered strong, since the integrated designs had better performance at a higher weight than the iterative designs. The results for the very weak thermal strengths of 0.9 and 1m/s indicate a modest performance increase at a reduced weight for the integrated designs, with the more pronounced effect at the lowest thermal strength. This was expected, since the intent of this investigation was to study a design process where reduced weight is an important consideration. The results in Table 6 do indicate the sensitivity of the design process to the thermal strength. Practical sailplane designs should be optimized over a range of thermal conditions.

The two design procedures each required about the same amount of computational time, approximately 900 s on an IBM 3084. This time is based on the iterative, sequential design requiring about four or five iterations. The proximity of the initial guess for the weight to the converged result greatly affected convergence of the iterative procedure. In all the cases presented in this paper, the initial guess for the weight was usually within 10% of the final weight. However, in general, the iterative, sequential design will require more CPU time than the integrated design.

V. Conclusions

Our investigation of the design process of a composite sailplane wing clearly demonstrates the superiority of an integrated design approach over an iterative, sequential procedure. Within the assumptions of very rudimentary aerodynamic and structural analyses, the integrated optimization procedure yielded superior designs. The integrated procedure was able to capitalize on favorable interactions between the aerodynamics and the structure. These interactions included distributing structural material so the deformations did not reduce aerodynamic performance and reducing the weight of the wing to increase the overall performance. Wing structural weight was reduced by concentrating more of the lift inboard and by reducing the planform area of the wing, resulting in lower root bending moments. The reduced weight was accompanied by reduced torsional stiffness and greater deformations. However, this did not depreciate the aerodynamic performance because the added deformations were compensated for by adding twist and distributing the structural material prudently. The separation of the two disciplines in the iterative procedure did not allow such interactions to be taken into account and applied toward improvement of the design.

The next step in the formulation of a complete integrated design process is to allow a more arbitrary wing shape and to use more exact methods for analyzing the aerodynamics and the structures. An arbitrary wing would include chord length and twist variations at each station and the addition of the thickness distribution of the airfoil section profile at each station as a design variable. A more exact aerodynamic analysis would entail using something such as vortex panel methods to obtain lift distribution and induced drag, with boundary-layer analysis to account for skin friction and form drag. The next step in the structural analysis is to introduce a finite-element

model allowing more freedom and higher accuracy in the structural design.

To utilize these more complex analysis techniques for an aircraft wing with an increased number of design variables and constraints would stretch the limits of today's supercomputers. If an entire aircraft and all its systems were included, the time required for a complete optimization would become impractical with existing computers. However, the present study does indicate that the benefits of an integrated multidisciplinary design process will make working toward a useful design procedure in the future very worthwhile.

Acknowledgment

This research was supported by NASA Langley Research Center under grants NAG1-505 and NAG1-603.

References

[1]Lynch, R. W. and Rogers, W. A., "Aeroelastic Tailoring of Composite Materials to Improve Performance," *Proceedings of the AIAA/ASME/SAE Structures, Structural Dynamics, and Materials*, King of Prussia, PA, May 1976.

[2]Haftka, R. T., "Optimization of Flexible Wing Structures Subject to Strength and Induced Drag Constraints," *AIAA Journal*, Vol. 15, No. 8, 1977, pp. 1101–1106.

[3]Ashley, H., "On Making Things the Best—Aeronautical Uses of Optimization," *Journal of Aircraft*, Vol. 19, No. 1, 1982, pp. 5–28.

[4]Haftka, R. T., "Structural Shape Optimization with Aeroelastic Constraints—A Survey of US Applications," *Journal of Vehicle Design*, Vol. 7, 1986, pp. 381–392.

[5]McGeer, T., "Wing Design for Minimum Drag and Practical Constraints," Ph.D. Thesis, Stanford Univ., 1984.

[6]Helwig, H. G., "Capglide and the RP-1," *Soaring*, Feb. 1980, pp. 22–25.

[7]Winkler, S. J., "Aeroelastic Analysis of a Composite Wing," M.S. Thesis, Rensselaer Polytechnic Inst., 1981.

[8]Winkler, S. J. and Bundy, F. P., "Rensselaer's 'Homebuilt' RP-2," *Soaring*, June 1983, pp. 26–29.

[9]Helwig, G., "Wing Shape Optimization for Maximum Cross-Country Speed with Mathematical Programming," N79-23899, Rensselaer Polytechnic Inst., 1979.

[10]Bertin, J. J. and Smith, M. L., *Aerodynamics for Engineers*, Prentice Hall, Englewood Cliffs, NJ, 1979.

[11]Bisplinghoff, R. L., Ashley, H., and Hoffman, R. L., *Aeroelasticity* Addison-Wesley, Reading, MA, 1955.

[12]Grandhi, R. V., Thareja, R., and Haftka, R. T., "NEWSUMT-A: A General Purpose Program for Constrained Optimization Using Constraint Approximations," *ASME Journal of Mechanisms, Transmission and Automation in Design*, March 1985, pp. 91–99.

[13]Thareja, R. and Haftka, R. T., "NEWSUMT-A: A Modified Version of NEWSUMT for Inequality and Equality Constraints," Rept. 148, VPI&SU, March 1985.